Düzce Üniversitesi Bilim ve Teknoloji Dergisi

Araştırma Makalesi

Numerical Investigation of the Effect of Cooling and Heating Conditions on the Performance of Thermoelectric Module

Seyda ÖZBEKTAŞ [a], Bilal SUNGUR [b,*], Bahattin TOPALOĞLU [a]

[a] *Department of Mechanical Engineering, Faculty of Engineering, Ondokuz Mayıs University, Samsun, TÜRKİYE*

[b] *Department of Mechanical Engineering, Faculty of Engineering, Samsun University, Samsun, TÜRKİYE*

* *Sorumlu yazarın e-posta adresi: bilal.sungur@samsun.edu.tr*

DOI: 10.29130/dubited.742775

ABSTRACT

Today, the need for energy increases, and fossil fuel resources run out rapidly so energy costs also increase rapidly. The most important feature of fossil fuels is that they consist of hydrocarbon and organic substances containing high levels of carbon. This causes great harm to the world and humanity. In the face of this dangerous situation, world states look for new and clean energy sources. As a result, the trend towards renewable energy sources increases rapidly. In this context, TE (thermoelectric) module is an important source to convert heat to electrical energy. The amount of electricity generation from heat depends on the temperature difference between surfaces of the TE module. The electrical power obtained from heat increases with the increase of temperature difference. This work aims to investigate numerically the heat transfer and electricity generation performance of a Bi_2Te_3-based TE module embedded with cylindrical pin-fin heat sink under the different hot surface and air temperature conditions with different air velocities. The results were evaluated and discussed with parameters such as temperature distribution, power input, power output, voltage output, current output, temperature difference, total thermal resistance, conversion efficiency and Nusselt number according to Reynolds numbers. In all analyses, it was observed that performance of the heat transfer and electricity generation of the TE module increase with the increase in Reynolds number. The highest conversion efficiency was obtained generally at surface temperatures of 200℃, specifically at air temperature of 5℃ and the Reynolds number of 20000. In addition, it was observed that the temperature difference between the surfaces of the TE module is not sufficient alone to give good performance and besides, it is necessary to keep the cold surface at low temperature.

Keywords: *Thermoelectric module, Heat sink, Numerical modelling, Electricity generation*

Soğutma ve Isıtma Şartlarının Termoelektrik Modülün Performansına Etkisinin Nümerik İncelenmesi

ÖZET

Günümüzde enerjiye olan talep artmaktadır ve fosil yakıt kaynakları hızla tükenmektedir, bunun sonucunda enerji maliyetleri de hızla artmaktadır. Fosil yakıtların en önemli özelliği, yüksek karbon seviyeleri içeren hidrokarbon ve organik maddelerden oluşmasıdır. Bu dünya ve insanlık için büyük zarara sebep olmaktadır. Bu tehlikeli durumun karşısında, dünya devletleri yeni ve temiz enerji kaynakları aramaktadırlar. Sonuç olarak, yenilenebilir enerji kaynaklarına yönelim hızla artmaktadır. Bu bağlamda termoelektrik (TE) modül, ısının elektrik enerjisine dönüşümünde önemli bir kaynaktır. Isıdan elektrik üretimi miktarı TE modülün yüzeyleri arasındaki sıcaklık farkına bağlıdır. Sıcaklık farkı arttıkça, ısıdan elde edilen elektriksel güç de artmaktadır. Bu çalışma farklı hava hızları, yüzey sıcaklıkları ve hava sıcaklıkları koşullarında, silindirik iğne kanatlı ısı alıcı gömülü bir Bi_2Te_3 TE modülünün ısı transferi ve elektrik üretimi performansı nümerik olarak incelemeyi

Geliş: 26/05/2020, Düzeltme: 10/08/2020, Kabul: 12/08/2020

amaçlamaktadır. Sonuçlar Reynolds sayısına göre, sıcaklık dağılımı, güç girdisi, güç çıktısı, gerilim çıktısı, akım çıktısı, sıcaklık farkı, toplam termal direnci, dönüşüm verimliliği ve Nusselt sayısı gibi parametrelerle değerlendirilmiş ve tartışılmıştır. Tüm analizlerde Reynolds sayısındaki artışla birlikte TE modülün ısı transferi ve elektrik üretimi performansının arttığı gözlemlenmiştir. En yüksek dönüşüm verimliliği genel olarak 200℃ yüzey sıcaklıklarında, spesifik olarak 20000 Reynolds sayısı ve 5℃ hava sıcaklığında elde edilmiştir. Ek olarak, TE modülün yüzeyleri arasındaki sıcaklık farkının iyi performans vermek için tek başına yeterli olmadığı bunun yanında soğuk yüzeyinin düşük sıcaklıkta tutulması gerektiği gözlemlenmiştir.

Anahtar Kelimeler: *Termoelektrik modül, Isı alıcı, Nümerik modelleme, Elektrik üretimi*

I. INTRODUCTION

Today, with the increase in the human population and the development of technology, energy sources are depleted rapidly and harmful gas emissions emitted by fossil fuel sources threaten the world. Additionally, nearly 70% of the world's energy is wasted as heat and released into the environment, causing global warming [1]. To prevent such disadvantages, the trend towards renewable energy sources has accelerated all over the world. The energy of waste heat released to the environment provides advantages because it is one of the clean, fuel-free and cheap energy sources. In this context, the thermoelectric (TE) module has an important place in collecting waste heat from industrial, residential and commercial fields and converting it into useful energy. It consists of a pair of P and N-type semiconductor legs that connected electrically in series and thermally in parallel, ceramic insulator plates and copper electrodes. P and N-type semiconductor legs have a positive Seebeck coefficient and negative Seebeck coefficient respectively. The scheme of electricity generation of the TE module is shown in Figure 1.

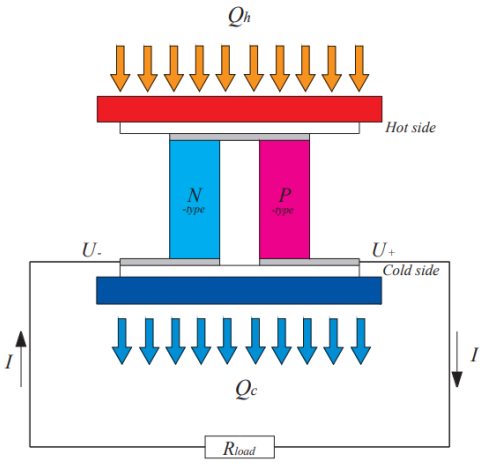

Figure 1. *Scheme of electricity generation of TE module*

TE modules work according to the Peltier and Seebeck effects. When a potential difference is applied to TE module, it works according to the Peltier effect and temperature difference occurs between its surfaces. When the temperature difference is created between its surfaces, it works according to the Seebeck effect and generates potential difference. In the Seebeck effect, a potential difference occurs between the circuit ends by applying different temperatures at the junction points of the materials A and B, which consist of different substances. Thermoelectric material must meet the following requirements: 1) High Seebeck coefficient leads to a high voltage and this is very important for increasing the energy conversion [2], 2) High electrical conductivity to reduce Joule heating due to the internal electrical losses [2], 3) Low thermal conductivity to conserve heat at the junctions, to allow a large temperature difference across the TEG, and to minimise thermal losses through the thermoelectric material [3].

TE modules have several advantages over traditional technologies and these advantages can be written as follows: simple structure, reliability, quiet and stable operation, no maintenance, no moving parts and long life. The main disadvantages of these modules are that it is inefficient and expensive [4].

TEG is used to recover waste heat at different powers (varying between μW and MW) and in different applications. Table 1 shows the temperature ranges and waste heat sources for TEG [5].

Table 1. *Temperature ranges and waste heat sources for TEG.*

Categories	**Heat Sources**	**Temperature** *(°C)*
Low temperature (< 230°C)	Cooling water from:	32–55
	Pumps and forming dies	27–88
	Air compressors	27–50
Medium temperature (230–650 °C)	Internal combustion engine exhausts	315–600
	Annealing furnace cooling systems	425–650
	Catalytic crackers	425–650
High temperature (> 650 °C)	Furnace (Aluminum refining)	650–760
	Cement kiln	620–730
	Furnace (Zinc refining)	760–110
	Furnace (Copper refining)	760–815

To increase the performance of TE module, heat sinks are often used. Heat sinks are cooling units that are used to lower the temperature of electronic devices, mostly by reducing the heat of the device with the help of a fan, preventing the device from overheating or burning. Besides, TEG can be created by connecting more than one TE modules electrically in series and parallel.

The literature review has been carried out on TE modules and heat sinks required for cooling the TE modules. Soleimani et al. [6] investigated numerically whether the power obtained from body temperature by using TE module can be used in the wearable personal heating system. The simulation was carried out using COMSOL Multiphysics software. To improve the performance of the TE module, four types of heat sink models at 0 m/s, 1.4 m/s, 3 m/s air velocities were compared with plate-fin heat sink which was the reference model. They concluded that all heat sink models have little effect on the power generation at the air velocity value of 0 m/s. Moreover, the four heat sink models at 1.4 m/s and 3 m/s air velocity performed significantly well compared to the plate-fin on TEG power generation. Luo et al. [7] researched the performance of the TEG system integrated with air and water by using the thermal resistance and numerical model. They concluded that the thermal resistance model gave acceptable results under appropriate conditions but numerical modeling could be used for more accurate results. Lv et al. [8] experimentally investigated the different types of heat exchangers to cool the cold side of the TE module. Calculations were concluded by considering the power consumption of the auxiliary equipment, costs and the powers obtained from TEG. The most useful heat exchanger was the finned heat sink because of simplicity and low price. However, the power output of this heat sink was poor. The water heat exchanger gave better power output due to the higher heat transfer coefficient of water compared to the air but it had lower efficiency and higher auxiliary equipment power consumption. As a result, it had been concluded that the heat exchanger with heat pipe obtained the best power output and net efficiency and it had lower auxiliary equipment power consumption and heat exchanger cost. Naphon et al. [9] experimentally and numerically investigated the cooling performance of the TE cooling module integrated with three different water block models which were named A, B and C. They concluded that numerical results were in reasonable agreement with the experimental results and the water block model C showed the best cooling performance among the other models. Erturun et al. [10] investigated numerically the mechanical and electrical performances of the TE module with different semiconductor leg geometries. They concluded that changes in power outputs, temperature distributions, and conversion efficiencies were limited for different leg geometries. Naphon and Wiriyasart [11] researched the liquid cooling which uses de-

ionized water in the fin heat sink which has rectangular geometry, with and without thermoelectric for CPU. They compared the results with the other cooling techniques. Huang et al. [12] studied the thermal influence of thermoelectric water-cooling equipment on an electronic device. They concluded that when the heat load is applied below 57 W, the cooling performance of conventional water-cooling devices can be improved by integrating thermoelectric coolers. Mostafavi and Mahmoudi [13] studied numerically and experimentally the TE generator system consisting of TE module, cold and hot side heat sinks. In their study, the hot side was heated by exhaust gas while the cold side was cooled by the air. As a result, for the same temperature difference, the highest practical and theoretical output powers were found 2.8 W and 3.4 W, respectively. Seo et al. [14] investigated numerically and experimentally a system consisting of TE modules integrated with heat sinks placed in a duct with square cross-section. They concluded that the performance of TE module significantly affected by the various parameters of the heat sinks integrated with the TE module. Du et al. [15] studied TEG system with exhaust-based which consist of TE modules, exhaust and cooling ducts. They observed the liquid cooling gave higher net power output compared to air cooling. Kiflemariam and Lin [16] aimed to cool the device without an external power source with the power obtained through thermoelectric generation from the heat of the device. They concluded that at optimum flow rate of cooling fluid, the heat source device temperature can be kept at the desired temperature while providing power to operate the coolant through a heat sink. Martine et al. [17] studied analytically and experimentally the concept of thermoelectric self-cooling. They proved experimentally that thermoelectric self-cooling technology increases the cooling performance of a device without an external power source. Joshi et al. [18] aimed to obtain water by condensing the moisture in the air with thermoelectric fresh water generator system. They observed that the quantity of water generated from moisture depended on air mass flow rate, electric current and humidity of moisture air. Sun et al. [19] investigated experimentally the TE cooling module integrated with a gravity assistant heat pipe (GAHP) and compared it with air-cooled heat sink. They observed that GAHP had better performance in term of the cooling capacity and electricity consumption. Liu et al. [20] used thermoelectric power generators to convert the automotive exhaust heat to electricity. As a result, they obtained power output of 944W and they stated that this kind of TE generator had significant potential for recover waste heat. Hsiao et al. [21] aimed to investigate the performance of a thermoelectric module in radiator and exhaust pipe of a vehicle. They concluded that the TE performance on the exhaust pipe was better than on the radiator. Li et al. [22] researched experimentally and numerically a TEG system consisting of a Bi_2Te_3-based TE module and two fluid heat exchangers. They observed that the fluid velocity had a significant effect on the temperature distribution. Wang et al. [23] aimed to compute the total power output and temperature distribution of an on-board automotive thermoelectric generator (ATEG) and compared the inserted fins with dimpled surface in the conventional hot heat exchanger. They concluded that dimpled surface ATEG had less pressure drop and more net power output than the ATEG installed. Chang et al. [24] experimentally investigated the TE air-cooling module and developed a theoretical model.

Studies generally focus on increasing electrical and heat transfer performance of the TE module using heat sinks with different geometries and materials, and liquid coolers with different materials. In this study, the thermal and electrical performance of TE module embedded with cylindrical pin-fin heat sink with different hot surface and air temperature conditions with different air velocities were investigated numerically. To model the turbulent flow, RNG k-Ɛ model was used. Under these conditions, calculations were realised for different Reynolds numbers. Results were evaluated as temperature, power input, power output and Nusselt numbers in relation to Reynolds number.

II. MATERIALS AND METHODS

A. MATHEMATICAL MODEL

Turbulent flows can be modeled using the finite volume method with Computational Fluid Dynamics (CFD) programs. In calculation of flow problems, mass, momentum and energy conservation

equations need to be solved. These differential equations are solved using boundary conditions suitable for problems. For turbulent steady-state flow, time-averaged continuity, momentum and energy equations were expressed as follows:

$$\frac{\partial U_i}{\partial x_i} = 0 \tag{1}$$

$$U_j \frac{\partial U_i}{\partial x_j} = \frac{\partial}{\partial x_j}\left(\nu \frac{\partial U_i}{\partial x_j} - \overline{u_\iota u_j}\right) - \frac{1}{\rho}\frac{\partial P}{\partial x_i} \tag{2}$$

$$U_j \frac{\partial T}{\partial x_j} = \frac{\partial}{\partial x_j}\left(\alpha \frac{\partial U_i}{\partial x_j} - \overline{u_j t}\right) \tag{3}$$

In these equations, U_i, is the mean-velocity vector, P is the mean static pressure, ρ is the fluid density and ν is the fluids kinematic viscosity. Reynolds stresses $(\overline{u_\iota u_j})$ in momentum conservation equation is defined by

$$-\overline{u_\iota u_j} = \nu_t \left(\frac{\partial U_i}{\partial x_j} + \frac{\partial U_j}{\partial x_i}\right) - \frac{2}{3}\delta_{ij}k \tag{4}$$

where ν_t is turbulent viscosity and defined as:

$$\nu_t = C_\mu \frac{k^2}{\varepsilon} \tag{5}$$

where k is the turbulent kinetic energy and ε is turbulent dissipation rate.
Turbulent heat flux in the conservation equation of energy $\left(\overline{\mathrm{u_j t}}\right)$ defined as:

$$\left(\overline{\mathrm{u_j t}}\right) = \alpha_\mathrm{t} \frac{\partial \mathrm{T}}{\partial \mathrm{x_j}} \tag{6}$$

where α_t is turbulence heat dissipation coefficient and defined as:

$$\alpha_\mathrm{t} = \frac{\nu_\mathrm{t}}{\mathrm{Pr_t}} \tag{7}$$

where $\mathrm{Pr_t}$ is turbulence Prandtl number."

In addition to the CFD analysis, the following equations are used for Thermal-Electric analysis [7]. Energy conservation equations used for P and N-type semiconductor legs in Thermal-Electric analysis are given in Eq. (8) and Eq. (9).

$$\nabla \cdot \left(\lambda_p(T)\nabla T_p\right) = -\sigma_p^{-1}(T)J^2 + \nabla\alpha_p(T)JT_p \tag{8}$$

$$\nabla \cdot \left(\lambda_n(T)\nabla T_n\right) = -\sigma_n^{-1}(T)J^2 + \nabla\alpha_n(T)JT_n \tag{9}$$

In Eq. (2) and Eq. (3), $\alpha_{p,n}(T)$, $\sigma_{p,n}^{-1}(T)$ and $\lambda_{p,n}(T)$ represent the Seebeck coefficient, electrical resistivity and the thermal conductivity of the P and N type semiconductor leg, respectively, and the current density vector is defined as J. The terms of $\nabla \cdot \left(\lambda_{p,n}(T)\nabla T_{p,n}\right)$, $-\sigma_{p,n}^{-1}(T)J^2$, $\nabla\alpha_{p,n}(T)JT_{p,n}$ correspond the Fourier heat, the Joule heat and the Peltier or Thomson heat, respectively.

The copper material has Joule effect but no Seebeck effect. Besides, ceramic material has neither Joule effect nor Seebeck effect. Therefore, for copper electrodes and ceramic plates differ from that of P and N semiconductor legs, and the energy conservation equations can be written as in Eq. (10) and Eq. (11), respectively.

$$\nabla \cdot (\lambda_{co} \nabla T) = -\sigma_{co}^{-1} J^2 \tag{10}$$

$$\nabla \cdot (\lambda_{ce} \nabla T) = 0 \tag{11}$$

In Eq. (4) and Eq. (5), σ_{co}^{-1}, λ_{co}, λ_{ce} represent the electrical resistivity and thermal conductivity of copper electrode, and thermal conductivity of ceramic plate, respectively.

The electric field intensity vector in semiconductor legs is given in Eq. (12).

$$E = -\nabla \varphi + \alpha \nabla T \tag{12}$$

In Eq. (12), the Seebeck electric motive force and the electric potential are shown as $\alpha \nabla T$ and φ, respectively.

Thus, using the Eq. (13), the current density vector in Eq. (8), Eq. (9) and Eq. (10) can be found.

$$J = \sigma E \tag{13}$$

Also, the current through the load resistance, semiconductor legs and copper electrodes is continuous and it can be shown as in Eq. (14).

$$\nabla J = 0 \tag{14}$$

By solving the above CFD and Thermal-Electric model, the thermal and electrical outputs of the TE module can be found. The input heat (Q_h) and current(I) are calculated on a selected cross-section by simple area integration of the heat flux and current density, respectively. Besides, the output power (P) is calculated according to the formula $= I^2 R_L$, and conversion efficiency from heat to electric can be found from Eq. (15).

$$\eta = \frac{P}{Q_h} = \frac{I^2 R_L}{Q_h} \tag{15}$$

B. BOUNDARY CONDITIONS AND SOLVER

In this work, thermal and electrical analysis of a TE module embedded with cylindrical pin-fin heat sink at the different surface and air temperatures with different air velocities were investigated numerically. It was assumed that material properties change both in thermal and electrical analysis depending on the temperature. Thermal analyses were realized with ANSYS Fluent which is CFD program. The heat applied to the surface of TE module is transferred from heat sink to air through conduction and convection. Air enters 3 mm above the heat sink and through a 38 mm circular cross-section and exits from four side surfaces of the cubic air domain. For numerical solution, suitable boundary conditions for inlet velocity and temperature must be given. Inlet velocities of air normal to the circular cross-section are specified according to Reynolds numbers at 5000, 10000, 15000 and 20000. The hot surface of TE module is set as wall boundary condition and the temperature values of this wall were 100°C, 200°C and 300°C. In addition, temperature values of air were 5°C, 15°C and 25°C. The heat transfer on the side surfaces of components of TE module and base of the heat sink is negligible so these surfaces set as adiabatic wall. Steady-state pressure-based solver has been employed for numerical solution. RNG k-ε model is used as turbulence model.

RNG k-ε model is obtained from the instantaneous Navier-Stokes equations by using Renormalization group methods. k and ε are obtained from the following transport equations which were described for RNG model.

$$\frac{\partial}{\partial t}(\rho k)+\frac{\partial}{\partial x_i}(\rho u_i k)=\frac{\partial}{\partial x_j}\left(\alpha_k \mu_{eff}\frac{\partial k}{\partial x_j}\right)+G_k+G_b-\rho\varepsilon-Y_M+S_k \tag{16}$$

$$\frac{\partial}{\partial t}(\rho \varepsilon)+\frac{\partial}{\partial x_i}(\rho u_i \varepsilon)=\frac{\partial}{\partial x_j}\left(\alpha_\varepsilon \mu_{eff}\frac{\partial \varepsilon}{\partial x_j}\right)-C_{2\varepsilon}\rho\frac{\varepsilon^2}{k}+C_{1\varepsilon}\frac{\varepsilon}{k}(G_k+C_{3\varepsilon}G_b)-R_\varepsilon+S_\varepsilon \tag{17}$$

where, α_k and α_ε represent the reverse effective Prandtl numbers of k and μ_{eff}, represents the effective (turbulent) viscosity. The constant values used in the RNG k-ε model are given in Table 2 [25].

Table 2. *The constants of RNG k-ε model*

Constant	Value
$C_{1\varepsilon}$	1.42
$C_{2\varepsilon}$	1.68
C_μ	0.0845
η_0	4.38
β	0.012
α_k	1.393
α_ε	1.393

For pressure-velocity coupling, SIMPLE algorithm is used. Convergence criteria for all the equations set to 10^{-6} except energy equation which is set to 10^{-5}. After thermal analysis had finished, the electrical analysis of TE module was realised. ANSYS Thermal-Electric program is employed for electrical analysis. The cold surface temperature of TE module which is a result of CFD program is imported to Thermal-Electric program. Unlike thermal analysis, a load resistance (R_L) is connected to the TE module in electrical analysis. Load resistance is chosen 3.5 Ω to give maximum power output to be taken from TE module. To provide this load resistance value, electrical resistivity of the part to be used as the load resistance is determined by using formula "$R_L = \sigma \cdot L/A$" where σ, L and A are electrical resistivity, length and sectional area of the part, respectively. Output values for current, voltage, and power were obtained under these conditions.

C. GEOMETRY

Figure 2 shows the designed TE module embedded with cylindrical pin-fin heat sink. This design consists of ceramic insulator plate, copper electrode, N and P-type semiconductor legs, cylindrical pin-fin heat sink and air domain. The dimensions and numbers of components of TE module are shown in Table 3. The cold surface of TE module is cooled by air and the cooling amount is increased with cylindrical pin-fin heat sink which is made of aluminium. As mentioned above, the air enters through a circular cross-section and exits from the four side surfaces of cubic air domain. Besides, the heat is applied to the hot surface of TE module.

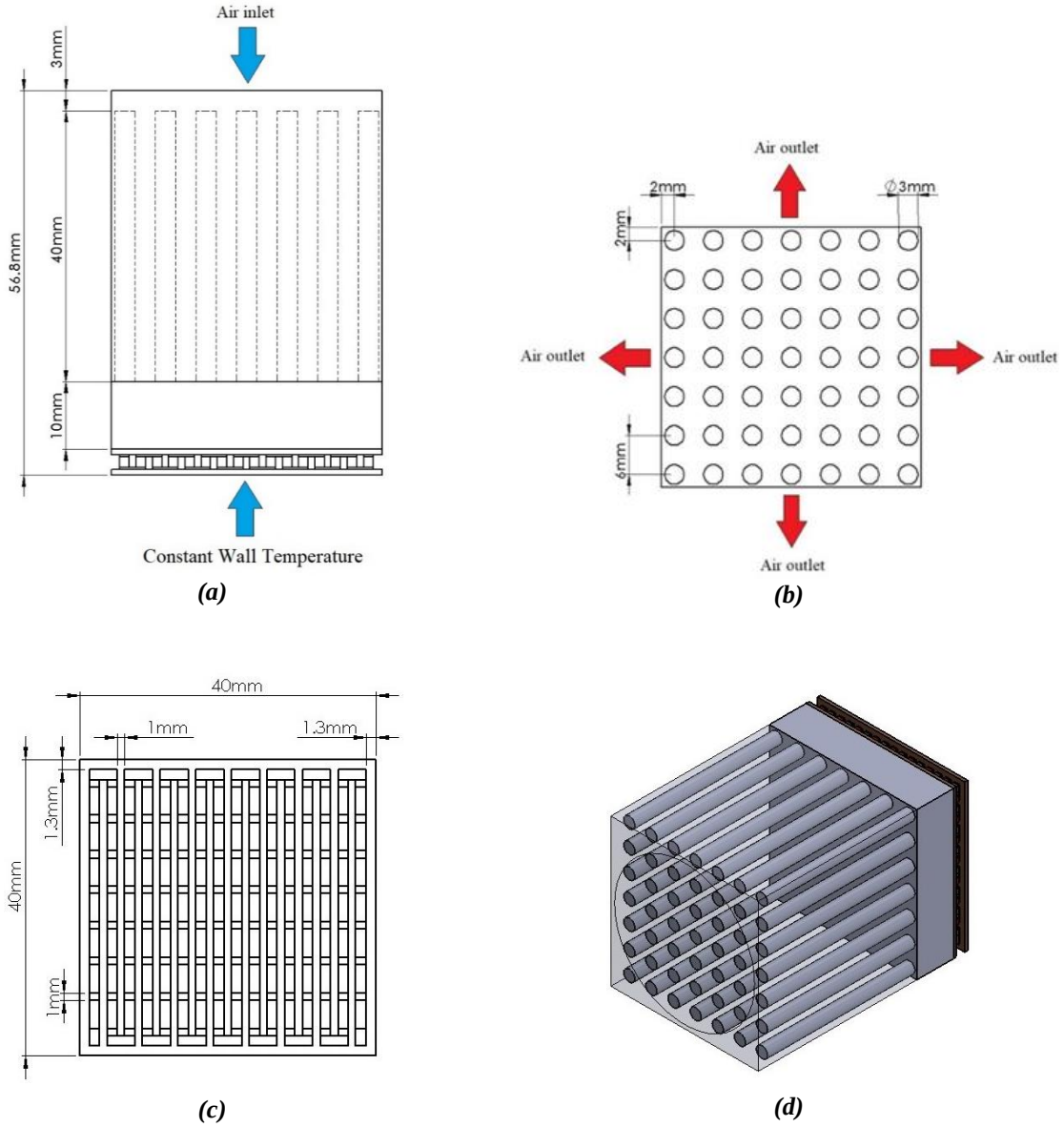

Figure 2. *The schematic of the TE module system.* ***(a)*** *The front view of the TE module system.* ***(b)*** *The top view of the cylindrical pin-fin heat sink.* ***(c)*** *The inside view of the TE module.* ***(d)*** *The perspective view of the TE module system*

Table 3. *Dimension and number of parts composing TE module*

Names	**Number of parts**	**Dimension** *(mm)*
Ceramic plate	2	40x40x0.8
Copper electrode	255	3.8x1.4x0.3
N-type leg	127	1.4x1.4x1.6
P-type leg	127	1.4x1.4x1.6

D. GRID STRUCTURE AND MATERIAL PROPERTIES

The geometry must be meshed before making a solution in CFD and Thermal-Electric analysis. The average skewness value between 0 and 0.25 and average orthogonal quality between 0.75 and 1 are acceptable mesh parameters [25]. The meshes used in this study were in this range. Mixed elements have been employed in the meshing process. This mesh has 4176533 number of elements. Also,

various mesh sizes, coarse, medium and fine meshes were tested to determine the grid-independent solution. Results of medium and fine meshes were close to each other and for this reason, the medium mesh was used in this study to save computation time. The grid structure of geometry is shown in Figure 3. The properties of materials are shown in Table 4. These properties are selected as temperature-dependent to obtain more accurate results. The material properties of the Bi_2Te_3-based TE module were taken from the study of Luo et al. [7].

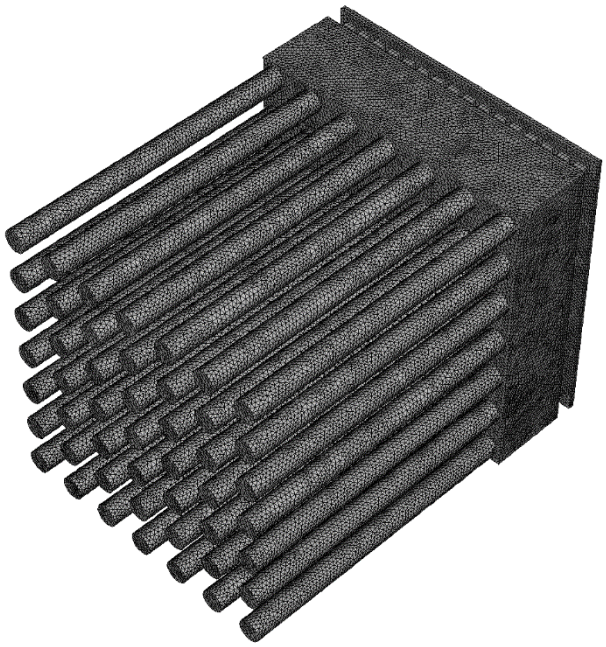

Figure 3. *The mesh structure of the TE module embedded with cylindrical pin-fin heat sink.*

Table 4. *Properties of the material of parts used in the analysis*

Names	**Seebeck coefficient** α $(\mu V \cdot K^{-1})$	**Electrical resistivity** σ $(10^{-5}\Omega \cdot m)$	**Thermal conductivity** λ $(W \cdot m^{-1} \cdot K^{-1})$	**Density** ρ (kg/m^3)	**Specific heat** c_p $(J/kg \cdot K)$
Ceramic plates	NA	NA	18	3690	880
Copper electrodes	NA	$7\times 10^{-6}T + 0.0015$	387.6	8978	381
P-type leg	$-0.00424T^2 + 3.01636T - 305.16$	$-1.3348 \times 10^{-5}T^2 + 0.01748T - 2.9564$	$4.8482 \times 10^{-5}T^2 - 0.0332T + 6.949$	6858	154
N-type leg	$0.00203T^2 - 1.40396T - 23.98$	$-1.6384 \times 10^{-5}T^2 + 0.01681T - 2.61$	$3.07 \times 10^{-5}T^2 - 0.02031T + 4.722$	7858	154
Heat sink	NA	NA	202.4	2719	871
Air	NA	NA	0.0242	1.225	1006.43

III. RESULTS AND DISCUSSIONS

In this work, calculations were carried out for 36 different situations using three different HST (Hot Surface Temperatures) (HST100, HST200, HST300), three different AT (Air Temperatures) (AT5,

AT15, AT25) and four different air velocities (Reynolds=5000, 10000,15000,20000). HST and AT represent hot surface temperatures and air temperature, respectively. The numbers coming after the hot surface temperatures (HST) and air temperatures (AT) show the temperature value. To obtain maximum power output from the TE module, 3.5 ohm load resistance of the same size as the internal resistance of the module was connected to the TE module.

The heat applied to the surface of TE module is transferred from heat sink to air through conduction and convection. This process was illustrated in Figure 4. Heat transfer performance by convection depends on mass flow, temperature and area. In addition, heat transfer performance by conduction depends on fin number, fin length, fin thickness and base thickness.

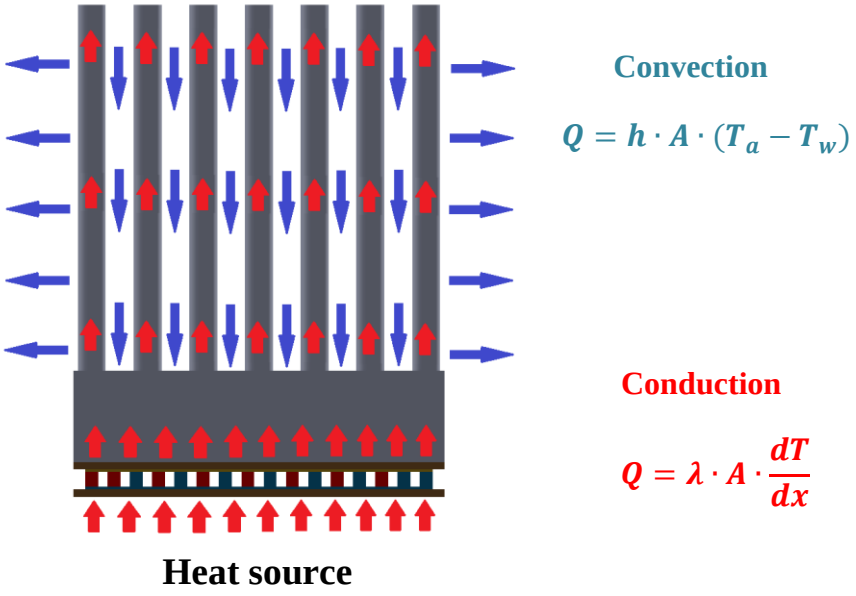

Figure 4. *Heat transfer process of the TE module embedded with cylindrical pin-fin heat sink*

It was observed that TE module has the highest conversion efficiency under conditions of the HST200, AT5 and Reynolds number of 20000. The temperature contours and velocity streamlines of the TE module under these conditions were shown in Figure 5. The temperature contours in Figure 5 (a) show the temperature of the cylindrical pin fins in the corner of the heat sink was lower compared to those in the centre because the air enters from a circular cross-section and the centre of the heat sink. The average temperatures of the cylindrical pin fins in the corner and centre of the heat sink was 29℃ and 22℃, respectively. As a result, there was an average temperature difference of 7℃ between them. The local temperature contours of the TE module in Figure 5 (b) shows that when the hot surface temperature was exposed to a temperature of 200℃, the cold surface of the TE module cooled down up to 43℃ under the influence of the p and n semiconductors with low thermal conductivity and heat sink, resulting in a temperature difference of approximately 157℃ between its surfaces. The local temperature contours of the air domain in three different cross-sections in Figure 5 (c) show that the air temperature rise towards the base of heat sink under cylindrical pin fins. As the Reynolds number increased, the air temperature decreased due to rapid air flow. As a result, the faster air flow provided better cooling. The velocity streamlines in Figure 5 (d) show that the air distributed smoothly between the cylindrical pin fins. Besides, it was observed that the air velocity increased between the cylindrical pin fins and decreased towards the outlets and the base of the heat sink.

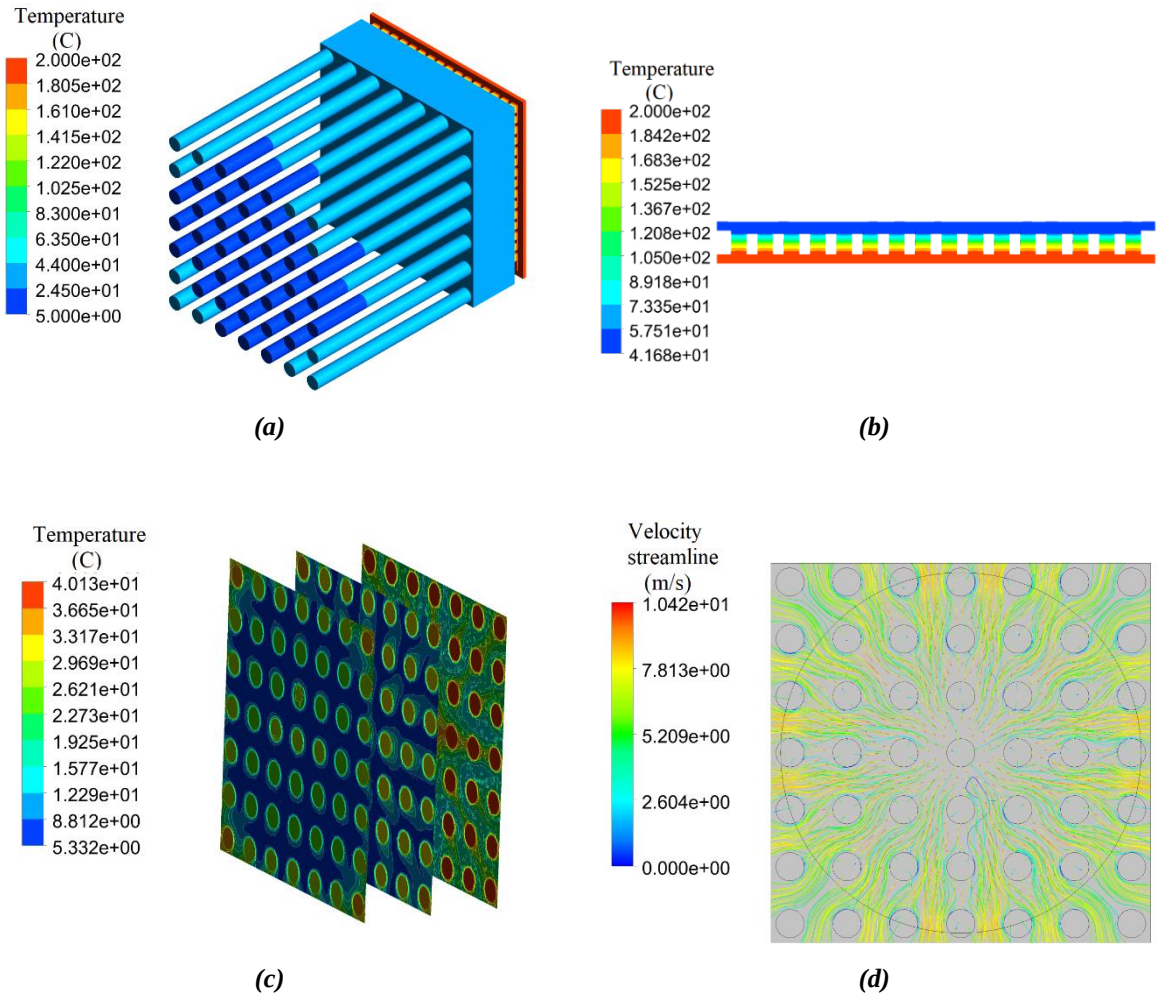

Figure 5. *The CFD analysis results of the TE module system under the conditions of HST200, AT5 and Reynolds number of 20000.* ***(a)*** *Global temperature contours of the TE module system.* ***(b)*** *Local temperature contours of the TE module.* ***(c)*** *Local temperature contours of the air domain in three different cross-sections.* ***(d)*** *Velocity streamlines of the air domain*

In Figure 6, global temperature contours of the TE module system at air temperature of 15°C with different Reynolds numbers and hot surface temperatures were given. The figure shows that when the Reynolds number increased, better cooling was observed. Also, the temperature values of the pin-fins in the centre decreased effectively towards the ends of them in all cases. It can be said that the heat transfer from the corners of heat sink was more difficult compared to its centre due to circular cross-section from which air enters.

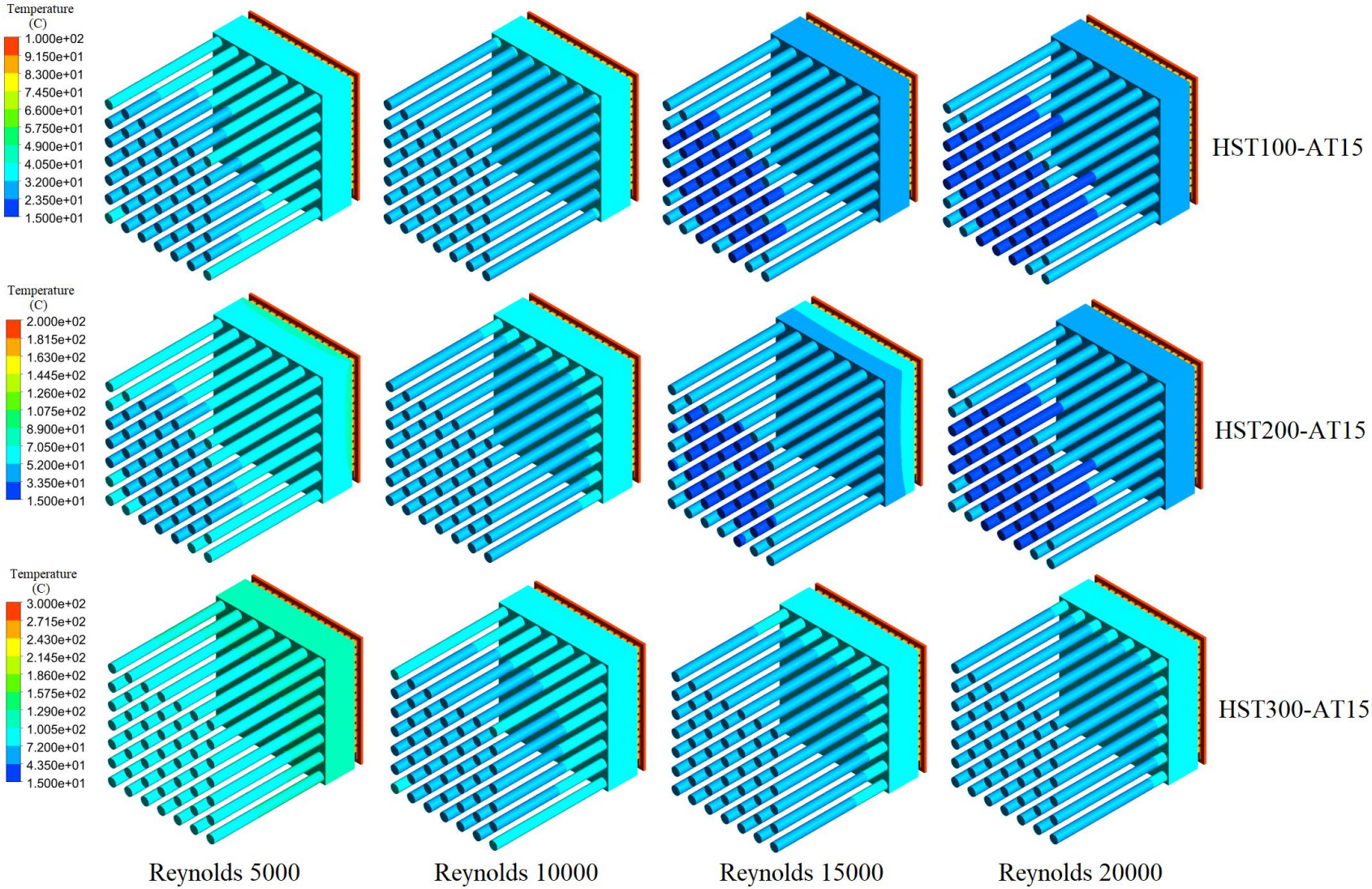

Figure 6. *Global temperature contours of the TE module system at air temperature of 15°C with different Reynolds numbers and hot surface temperatures*

The voltage and total current density distributions of the TE module under the conditions of HST200, AT5 and Reynolds number of 20000 where the highest electrical conversion efficiency occurred were given in Figure 7. According to the figure, the highest voltage output was 4.08V and the current density value in the cross-section of the copper electrode was 2775 mA/mm^2. Current output was obtained 1.16A when the current density was multiplied by cross-section of the copper electrode.

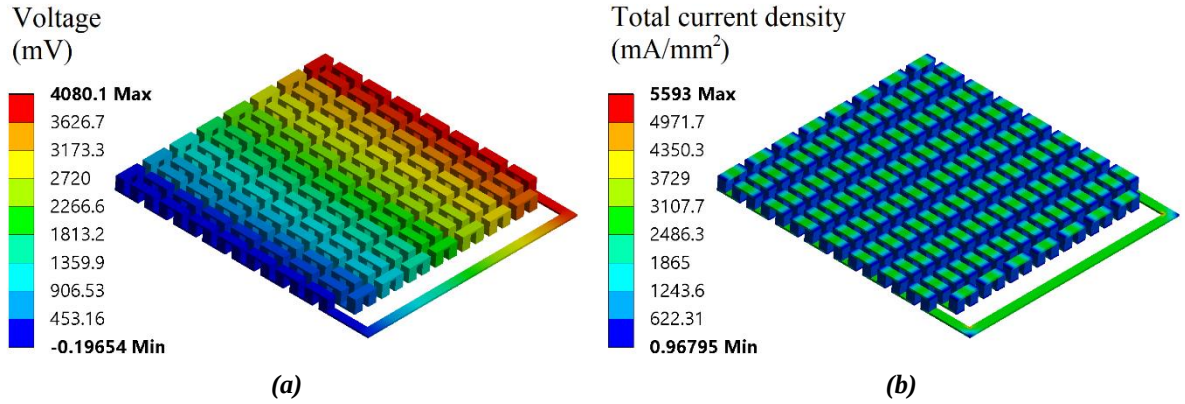

Figure 7. *The Thermal-Electric analysis results of the TE module system under the conditions of HST200, AT5 and Reynolds number of 20000.* ***(a)*** *Voltage distributions of TE module.* ***(b)*** *Total current density distributions of TE module.*

Graphics of the CFD and Thermal-Electric analysis results of the TE module system were given in Figure 8. Some terms were explained following. Power input is the amount of energy required to hold the hot surface of the TE module at a constant temperature. Power output is the amount of electrical energy obtained from the TE module to which heat is applied. The Nusselt number is a dimensionless number that expresses the ratio of the convection heat transfer coefficient to conduction heat transfer coefficient. Temperature difference is the difference between hot surface and cold surface of the TE module. The ratio of the temperature difference between the two faces of a material to the rate of heat flow per unit area is defined as thermal resistance. In addition, the total thermal resistance is the sum of the thermal resistance of all the elements of the TE module. The ratio of power output to power input is defined as conversion efficiency.

The highest conversion efficiency was obtained at HST200, AT5 and Reynolds number of 20000, while the lowest conversion efficiency was obtained at HST300, AT25 and Reynolds number of 5000. The highest conversion efficiency and the lowest conversion efficiency were calculated as 6.7% and 2.1%, respectively. The highest power input and output occurred at HST300, AT5 and Reynolds number of 20000, while the lowest power input and output occurred under the conditions of HST100, AT25 and Reynolds number of 5000. As result, the highest and the lowest power input were calculated as 134.6W and 21.7W, respectively. In addition, the highest and the lowest power output were 5.55W and 0.76W, respectively. This shows that the power input and output change proportional to the applied temperature difference. As an exception to this situation, in this work, the power outputs at HST300 and Reynolds number of 5000 was found lower than that at HST200 and Reynolds number of 5000. This is because the cold surface of the TE module is exposed to much higher temperature although the TE module at HST300 and Reynolds number of 5000 has higher temperature difference between its surfaces. Consequently, only high temperature difference is not enough for high power output. Besides, cold surface of the TE module must be kept at low temperatures. The current and voltage outputs also act similarly as power outputs. The highest output of current and voltage were 1.26A and 4.41V at HST300, AT5 and Reynolds number of 20000, respectively, while the lowest output of current and voltage were 0.46A and 1.64V at HST100, AT25 and Reynolds number of 5000, respectively. The highest temperature difference between surfaces of the TE module was 225°C at HST300, AT5 and Reynolds number of 20000, while the lowest temperature difference was 54°C at HST100, AT25 and Reynolds number of 5000.

As mentioned above, the high temperature difference is a desirable situation for a TE module. However, according to the results, although the highest temperature difference and power output occurred under the conditions of HST300 and AT5, the highest conversion efficiency was observed under the conditions of HST200 and AT5 because the power input to be applied for HST300 was much more than the power output obtained.

Total thermal resistance decreased as the Reynolds number increased. The highest thermal resistance was 3.49K/W at HST100, AT5 and Reynolds number of 5000, while the lowest thermal resistance was 2.13K/W at HST300, AT25 and Reynolds number of 20000. The highest Nusselt number occurred at HST300, AT25 and Reynolds number of 20000. On the other hand, the lowest Nusselt number occurred at HST100, AT5 and Reynolds number of 5000. The highest and the lowest Nusselt numbers were calculated as 12.49 and 5.20, respectively.

In all analyses, the power input and output, current output, voltage output, the conversion efficiency, the Nusselt number, and the temperature difference between surfaces of the TE module increased proportionally to increasing Reynolds number. However, this increase decreased gradually, as the Reynolds number increased.

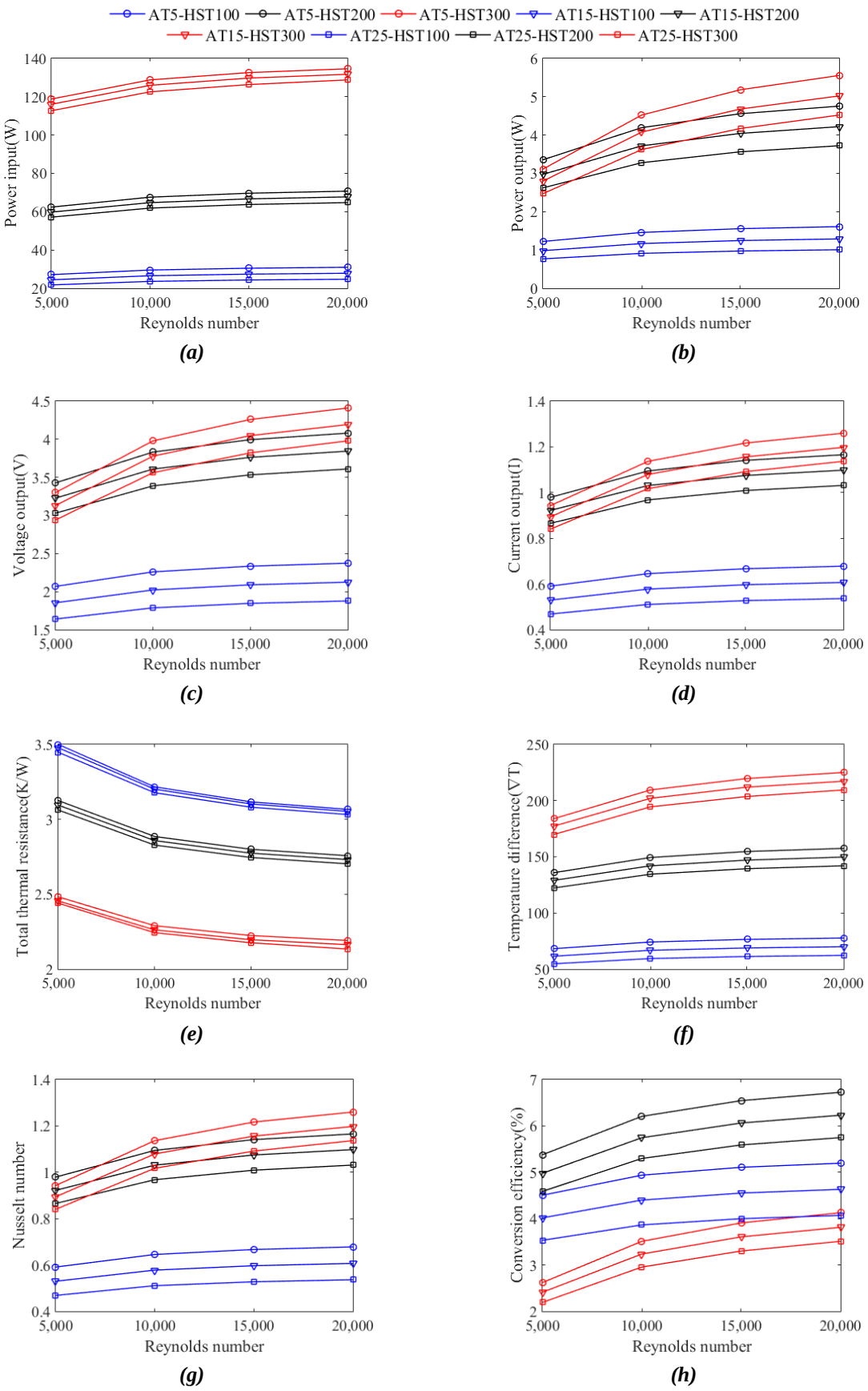

Figure 8. *Graphics of the CFD and Thermal-Electric analysis results of the TE module system.* ***(a)*** *Power input,* ***(b)*** *Power output,* ***(c)*** *Voltage output,* ***(d)*** *Current output,* ***(e)*** *Total thermal resistance,* ***(f)*** *Temperature difference,* ***(g)*** *Nusselt number,* ***(h)*** *Conversion efficiency in relation to Reynolds number*

IV. CONCLUSIONS

In this work, thermal and electrical performance of TE module embedded with cylindrical pin-fin heat sink was investigated numerically. The pin-fin heat sink was used to obtain higher efficiency by cooling the TE more effectively. In these analyses, the air is blown from a circular cross-section at different temperatures and velocities. In addition, different hot surface temperatures applied to the TE module. Calculations were made in three-dimensional conditions. To model the turbulent flow, RNG k-Ɛ model was used. Under these conditions, calculations have been made for different Reynolds numbers. Results have been evaluated as temperature contours, power input, power output, voltage output, current output, temperature difference, total thermal resistance, conversion efficiency and Nusselt number in relation to Reynolds numbers. The highest power input and output were under the conditions of HST300, AT5 and Reynolds number of 20000. The lowest conversion efficiency was found generally at HST300, specifically at AT25 and Reynolds number of 5000. In addition, the highest conversion efficiency was found generally at HST200, specifically at AT5 and Reynolds number of 20000. This shows that as the power input increases, the power output obtained by the TE module cannot catch up with this increase at the same rate and the conversion efficiency decreases. As mentioned above, the power outputs at HST300 and Reynolds number of 5000 was lower than expected because the TE module is exposed to high temperature and it cannot be cooled well. Also, the power input, power output, conversion efficiency, temperature difference and Nusselt number increased with increasing Reynolds number. On the other hand, total thermal resistance decreased with increasing Reynolds number. In future studies, the effect of different heat sink models and materials to the performance of a TE module can be researched.

V. REFERENCES

[1] R. Zevenhoven and A. Beyene, "The relative contribution of waste heat from power plants to global warming," *Energy*, vol. 36, no. 6, pp. 3754-3762, 2011.

[2] M. von Lukowicz, E. Abbe, T. Schmiel and M. Tajmar, "Thermoelectric generators on satellites—an approach for waste heat recovery in space," *Energies*, vol. 9, no. 7, p. 541, 2016.

[3] C. Goupil, W. Seifert, K. Zabrocki, E. Müller and G. Snyder, "Thermodynamics of thermoelectric phenomena and applications," *Entropy*, vol. 13, no. 8, pp. 1481-1517, 2011.

[4] U. Şahin, G. Coşkun, H. Soyhan, "Traktör egzozundan atılan ısı enerjisinin elektrik enerjisi olarak kazanımını sağlayan termoelektrik jeneratör," *Uluslararası Yakıtlar Yanma ve Yangın Dergisi*, s. 6, ss. 10-19, 2018.

[5] K. Zeb et al., "A survey on waste heat recovery: Electric power generation and potential prospects within Pakistan," *Renewable and Sustainable Energy Reviews*, vol. 75, pp. 1142-1155, 2017.

[6] Z. Soleimani, S. Zoras, Y. Cui, B. Ceranic and S. Shahzad, "Design of heat sinks for wearable thermoelectric generators to power personal heating garments: A numerical study," *IOP Conference Series: Earth and Environmental Science*, vol. 410, p. 012096, 2020.

[7] D. Luo, R. Wang and W. Yu, "Comparison and parametric study of two theoretical modeling approaches based on an air-to-water thermoelectric generator system," *Journal of Power Sources*, vol. 439, p. 227069, 2019.

[8] S. Lv et al., "Study of different heat exchange technologies influence on the performance of thermoelectric generators," *Energy Conversion and Management*, vol. 156, pp. 167-177, 2018.

[9] P. Naphon, S. Wiriyasart and C. Hommalee, “Experimental and numerical study on thermoelectric liquid cooling module performance with different heat sink configurations,” *Heat and Mass Transfer*, vol. 55, no. 9, pp. 2445-2454, 2019.

[10] U. Erturun, K. Erermis and K. Mossi, “Effect of various leg geometries on thermo-mechanical and power generation performance of thermoelectric devices,” *Applied Thermal Engineering*, vol. 73, no. 1, pp. 128-141, 2014.

[11] P. Naphon and S. Wiriyasart, “Liquid cooling in the mini-rectangular fin heat sink with and without thermoelectric for CPU,” *International Communications in Heat and Mass Transfer*, vol. 36, no. 2, pp. 166-171, 2009.

[12] H. Huang, Y. Weng, Y. Chang, S. Chen and M. Ke, “Thermoelectric water-cooling device applied to electronic equipment,” *International Communications in Heat and Mass Transfer*, vol. 37, no. 2, pp. 140-146, 2010.

[13] S. Mostafavi and M. Mahmoudi, “Modeling and fabricating a prototype of a thermoelectric generator system of heat energy recovery from hot exhaust gases and evaluating the effects of important system parameters,” *Applied Thermal Engineering*, vol. 132, pp. 624-636, 2018.

[14] Y. Seo, M. Ha, S. Park, G. Lee, Y. Kim and Y. Park, “A numerical study on the performance of the thermoelectric module with different heat sink shapes,” *Applied Thermal Engineering*, vol. 128, pp. 1082-1094, 2018.

[15] Du, H. Diao, Z. Niu, G. Zhang, G. Shu and K. Jiao, “Effect of cooling design on the characteristics and performance of thermoelectric generator used for internal combustion engine,” *Energy Conversion and Management*, vol. 101, pp. 9-18, 2015.

[16] R. Kiflemariam and C. Lin, “Numerical simulation of integrated liquid cooling and thermoelectric generation for self-cooling of electronic devices,” *International Journal of Thermal Sciences*, vol. 94, pp. 193-203, 2015.

[17] A. Martínez, D. Astrain and A. Rodríguez, “Experimental and analytical study on thermoelectric self cooling of devices,” *Energy*, vol. 36, no. 8, pp. 5250-5260, 2011.

[18] V. Joshi, V. Joshi, H. Kothari, M. Mahajan, M. Chaudhari and K. Sant, “Experimental investigations on a portable fresh water generator using a thermoelectric cooler,” *Energy Procedia*, vol. 109, pp. 161-166, 2017.

[19] X. Sun et al., “Experimental research of a thermoelectric cooling system integrated with gravity assistant heat pipe for cooling electronic devices,” *Energy Procedia*, vol. 105, pp. 4909-4914, 2017.

[20] X. Liu, Y. Deng, Z. Li and C. Su, “Performance analysis of a waste heat recovery thermoelectric generation system for automotive application,” *Energy Conversion and Management*, vol. 90, pp. 121-127, 2015.

[21] Y. Hsiao, W. Chang and S. Chen, “A mathematic model of thermoelectric module with applications on waste heat recovery from automobile engine,” *Energy*, vol. 35, no. 3, pp. 1447-1454, 2010.

[22] W. Li et al., “The temperature distribution and electrical performance of fluid heat exchanger-based thermoelectric generator,” *Applied Thermal Engineering*, vol. 118, pp. 742-747, 2017.

[23] Y. Wang, S. Li, X. Xie, Y. Deng, X. Liu and C. Su, “Performance evaluation of an automotive thermoelectric generator with inserted fins or dimpled-surface hot heat exchanger,” *Applied Energy*, vol. 218, pp. 391-401, 2018.

[24] Y. Chang, C. Chang, M. Ke and S. Chen, “Thermoelectric air-cooling module for electronic devices,” *Applied Thermal Engineering*, vol. 29, no. 13, pp. 2731-2737, 2009.

[25] *Fluent User’s Guide*, Fluent Incorporated, Lebanon, NH, 2006.